



POLITECNICO DI TORINO
Repository ISTITUZIONALE

Innovative technique for the base isolation of existing buildings

Original

Innovative technique for the base isolation of existing buildings / DE STEFANO, Alessandro; Clemente, Paolo; INVERNIZZI, Stefano; MATTA, EMILIANO; QUATTRONE, ANTONINO. - ELETTRONICO. - 1(2015), pp. 377-387. ((Intervento presentato al convegno COMPDYN 2015 5th ECCOMAS Thematic Conference on Computational Methods in Structural Dynamics and Earthquake Engineering tenutosi a Crete island, Greece nel 25-27 May 2015.

Availability:

This version is available at: 11583/2641510 since: 2020-04-29T12:35:27Z

Publisher:

Institute of Structural Analysis and Antiseismic Research, School of Civil Engineering, National Technical

Published

DOI:

Terms of use:

openAccess

This article is made available under terms and conditions as specified in the corresponding bibliographic description in the repository

Publisher copyright

(Article begins on next page)

INNOVATIVE TECHNIQUE FOR THE BASE ISOLATION OF EXISTING BUILDINGS

Alessandro De Stefano¹, Paolo Clemente², Stefano Invernizzi³, Emiliano Matta³, Antonino Quattrone³

¹ Politecnico di Torino, C.so Duca degli Abruzzi 24, 10129, Turin, Italy
alessandro.destefano@polito.it

² ENEA, Via Anguillarese 301, 00123 Rome, Italy
paolo.clemente@enea.it

³ Politecnico di Torino, C.so Duca degli Abruzzi 24, 10129, Turin, Italy
stefano.invernizzi@polito.it, emiliano.matta@polito.it, antonino.quattrone@polito.it

Keywords: Monitoring; closely-spaced micro-tunnels; damage assessment; soil-structure interaction; base-isolation.

Abstract. *An innovative base isolation system has been recently proposed for the retrofitting of existing buildings, in which the isolation layer is inserted under the building foundations so that the building, along with its foundations, is isolated from the surrounding soil. The isolation layer resides in closely-spaced micro-tunnels, constructed under the entire width of the building. These micro-tunnels, along with the trenches around the building, isolate the structure from the surrounding soil. The execution of these micro-tunnels is the most critical construction stage, because it may result in settlements which can damage the structure. In this paper, the behaviour of an existing structure, consisting of a masonry wall subjected to tunnelling-induced ground subsidence, is analysed. A parametric study is conducted using 2-D nonlinear finite element analyses to understand the role of key factors such as strength and stiffness of soil and masonry, roughness of soil-structure interface, excavation sequence of tunnels, wall dimensions and openings configuration. The study identifies the design variables which influence the most the risk of structural damage and suggests the most effective damage symptoms to be monitored during construction.*

1 INTRODUCTION

The usual base isolation design to improve the seismic resistance of existing buildings leads to extensive and intrusive manipulations of the construction body that severely alter the original structural configuration, thus resulting generally inapplicable to historical constructions or whenever existing architectural features are of economic importance.

An innovative way of isolating buildings from seismic actions has been proposed by Clemente and De Stefano [1][2], which, unlike conventional methods, does not involve any modification of the existing structure. The method calls for isolation of the building along with its foundation soil from the rest of the ground and consists in executing a series of closely-spaced micro-tunnels under the building and in placing isolators within the thickness of the tunnels lining. The execution of micro-tunnels is the most critical construction stage of the proposed intervention, because it may result in settlements, and therefore can induce structural or non-structural damage into the building. In order to keep damage below the desired thresholds, it is of paramount importance to develop adequate analytical, numerical and empirical tools, which can accurately and reliably predict the effect of excavations, and execution procedures capable to minimize the expected damage. Furthermore, it is important to properly track, during construction, possible deviations between the expected and the actual response of the soil-structure system, so as to identify the necessary corrections, if needed, to the execution process (soil consolidation, modification of the tunnelling sequence, etc.).

Surface and subsurface ground subsidence accompanying tunnelling operation, as well as the effect of the tunnel-related ground subsidence on the structures on surface, have received attention in the form of empirical, numerical and analytical studies [3][4][5][6][7][8][9]. These studies refer to single tunnels only, and were subsequently extended to the case of multiple tunnels [10][11][12]. Researchers, such as Boscardian & Cording [13] and Burland & Wroth [6], identified damage indicators for structures undergoing tunnel-induced settlements and used them to establish several levels of damage-thresholds; they used average horizontal strain, angular distortion/strain and deflection ratio in their studies. Various case studies have been done in the past where the tunnelling-induced damage was anticipated in terms of damage-indicators; damage-thresholds were determined for them and building was monitored during tunnel construction, keeping those damage-thresholds in mind. Those studies involved cases where deformation caused by one tunnel was the main source of damage on the existing structure. No studies are reported, to the best of the authors' knowledge, regarding closely-spaced multiple tunnels like the one discussed in the present application and the correlated structural damage.

The present paper aims to investigate how closely-spaced micro-tunnelling can adversely affect the structural state of existing masonry buildings and how monitoring during construction can help to reduce the risk of unpredicted damage. To this purpose, accurate 2-D nonlinear analyses are performed, simulating the coupled soil-structure interaction problem during sequential micro-tunnelling execution. The influence of different design variables on the onset and development of structural damage (crack opening) is first studied, and design recommendations are formulated regarding the best procedures to adopt in executing closely-spaced micro-tunnels so as to minimize damage. Correlations are then searched for between the extent of damage and different damage-indicators, and recommendations are finally inferred as to which indicators should be observed during monitoring of tunnel-construction.

2 THE INNOVATIVE ISOLATION SYSTEM

The new solution proposed consists in the realization of an isolated platform under the foundations of the building, without touching the building itself. A discontinuity between the foundations and the soil is created by means of the insertion of horizontal pipes and the positioning of isolation devices at the horizontal diametric plane. Then the building is separated from the surrounding soil in order to allow the horizontal displacements required by the isolation system. So the structure is seismically isolated but not interested by interventions that could modify its architectural characteristics, which is very important for historical buildings but also for large structures such as industrial plants [14][15].

Even underground level are not modified but can be part of the seismically protected building. In more details the construction phases are the following:

- a trench is first excavated of at one side of the building and pipes are inserted by means of auger boring or micro-tunnelling technique; the diameter of pipes should be ≥ 2 m, in order to allow the inspection of the isolation system; the pieces of pipe should have a particular shape and are composed by two portions, the lower and the upper sectors, respectively, which are connected by means of removable elements.
- the connection elements placed in correspondence of the isolation devices are removed and each pipe is joined with the two adjacent ones, for example by means of a reinforced concrete elements;
- the isolation devices are positioned and the upper adjacent sectors are connected in correspondence of the isolators;
- successively also the other connection elements are removed, so the lower and upper sectors are definitely separated;
- finally vertical walls are built along the four sides of the building.

The construction phases could be preceded by a stiffening of the soil by using jet grouting technique or others. This allows avoiding collapses during the works and is absolutely due when the distance from close structures is low. The system allows also the realization of a tunnel for pedestrian or vehicles. The size of the pipes must guarantee the accessibility and the possibility to substitute the devices.

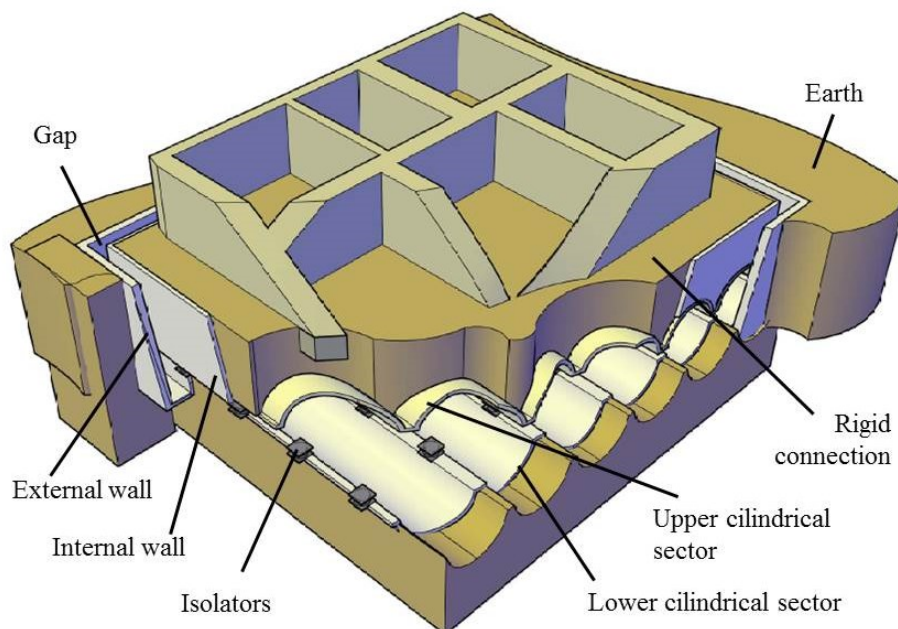


Figure 1 : The proposed method for seismic isolation

During the response to the earthquake the ground mass, added to the isolated structure as part of the mechanical system in relative motion with respect to the supporting ground, can play a positive role thanks to a more regular mass distribution and reduction of the overturning moment. It makes easy to obtain a very long fundamental period and, consequently, a large acceleration reduction. The trench surrounding the isolated structure, if necessary, can be used to install supplementary damping devices to keep under control the relative displacements.

The following chapter is devoted to the numerical settlement prediction during the construction of the micro-tunnels. A specific case study is explored in detail as a simulated experiment. Results are not fully extendable to every possible application, with different soil conditions, different building configurations and bore depth. In specific cases a previous mechanical improvement of the ground can be required. Anyway the numerical simulation can suggest some general conclusions

3 THE NUMERICAL MODEL

3.1 The baseline model

The 2-D numerical model used in the parametric study has been built using the commercial finite-element-method (FEM) software DIANA [16]. A general view of the model is reported in Figure 2, where two different opening configurations are exemplified, either with or without crack pattern and mesh discretization. Soil is modelled as a homogeneous, isotropic, linear-elastic perfectly-plastic material with Mohr-Coulomb yield surface and zero-tension cut-off. The soil is represented with 8-nodes quadrilateral plane-strain elements; few soil elements, inside and around excavation, are modelled as 6-nodes triangular plane-stress elements [17].

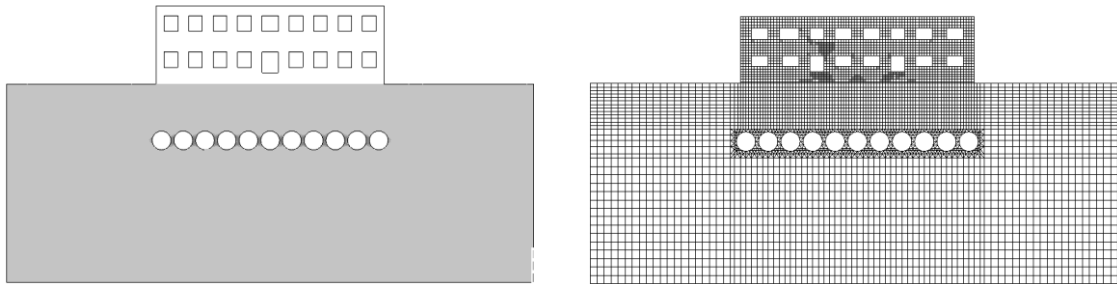


Figure 2 : The two different opening configurations for the 24.2 m long wall (1-Door on the left, 2-Door on the right), either with or without showing the final crack pattern and mesh discretization

Masonry is modelled as a homogeneous and isotropic material. A linear response is assumed for masonry in the elastic regime, while a smeared crack approach with strain decomposition is used to simulate its behaviour in cracking. A fixed-crack model with linear tension softening and constant tension cut-off criteria is used to simulate crack initiation and propagation (Figure 3). Masonry wall is modelled with 8-nodes quadrilateral plane-stress elements.

The interaction between soil and masonry is modelled through interface elements, relating normal and shear forces to normal and shear relative displacements across the interface. The values of interface stiffness are chosen such that the interface allows slip (tangential movement) between soil and masonry at very low shear stress. Interface is represented as 6-nodes line-interface elements.

The lining and the lintel are modelled as a linear-elastic, isotropic and homogeneous material; lining is represented as 3-nodes curved shell elements and lintel with 3-nodes 2-D beam elements. The bottom and lateral boundaries of soil are constrained in perpendicular direction;

top boundary is free to move in both directions. The model is loaded with gravity and superimposed loads, including dead and live loads acting on floors. In order to simplify the problem, dampers are not included in the model.

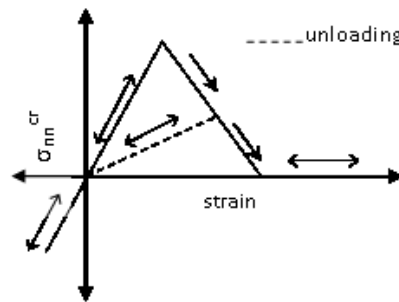


Figure 3 : Masonry constitutive law adopted in simulations

3.2 Modelling excavation process

Simulation of sequential tunneling obeys the following procedure. Initial soil stresses are established first, which are based on unit weight of soil and coefficient of earth pressure at rest; displacements are suppressed in this phase. Next step involves activation of masonry elements along with their self-weight and superimposed load. Then the excavation process modelled. Namely:

- Soil elements, corresponding to the first tunnel, are removed, and the model is allowed to establish equilibrium under gravity and superimposed loads. No internal pressure is applied on the periphery of excavation. DIANA's 'phased analysis' is used for this purpose.
- Soil elements, corresponding to the second tunnel, are then removed; lining elements are added around the first tunnel and the model is allowed to establish equilibrium under gravity and superimposed loads. No internal pressure is applied on the periphery of the excavation.
- The previous step is repeated for the remaining tunnels.

In the above steps, it is assumed that the "annular space" or the "gap" (i.e. the space between soil and lining) is the main source of volume loss, owing to the relatively stiffer soil conditions and small size of tunnel. Volume loss is simulated by allowing the tunnel to undergo instantaneous settlement, with no pressure applied on the excavated boundary, before the installation of lining elements. Since the introduction of the lining elements into the model prevents further closure of the gap, the model is meant to be representative of a real tunnelling process in which the gap must be completely filled with grout after installation of lining.

3.3 Wall configurations and excavation sequences in the parametric study

The parametric study has been conducted assuming three different values of the length of the masonry wall (24.2 m, 15.5 m, and 12.6 m) while keeping constant the height of the wall and the diameter (D) of the tunnels. Consequently, the number of tunnels required to cover each wall length are: 11 tunnels for the 24.2 m wall; 7 tunnels for the 15.5 m; and 6 tunnels for the 12.6 m wall.

Two types of opening configurations are considered for the 24.2 m wall, either 1-Door or 2-Door (Figure 2), while other walls are analysed with one type of opening configuration only. Three construction sequences are considered for the 11-tunnel assembly, three for the 7-tunnel assembly, one for the 6-tunnel assembly. The adopted sequences are shown in Figures 4 to 6. For all the models, soil bottom boundary is kept at $8D$ from the centre of tunnels, the side

boundary is kept at $8D$ from the centre of the outermost tunnels, and the depth of the centre of tunnels is chosen as 6 m for all models.

3.4 Geometric and material properties

Material properties adopted for soil and masonry are shown in Tables 1 and 2, where E is the elastic modulus, c is the cohesion, γ is the unit weight, ν is the Poisson's ratio, Ψ is the dilatancy angle, ϕ is the friction angle and K_o is the coefficient of lateral earth pressure at rest. Material parameters adopted for lining are: $\gamma = 24.5 \text{ kN/m}^3$, $E = 21 \text{ GPa}$, $\nu = 0.15$. For lintel, the same γ and ν are adopted as for lining, but E is reduced to 15 GPa. The normal stiffness of the interface elements is selected as $4 \times 10^8 \text{ N/m}^3$, while its tangential stiffness is 5 N/m^3 , as suggested by literature.

In all the models, the height and the thickness of the wall are kept at, respectively, 6.75 m and 0.22 m; the thickness of lining at 0.1 m; the cross-section of the lintel at $0.22 \times 0.16 \text{ m}$; the diameter of the tunnels at 2 m; and the distance between their centre at 2.2 m.

Tunnel assembly	E (MPa)	c (kPa)	γ (kN/m^3)	ν (-)	Ψ ($^\circ$)	ϕ ($^\circ$)	K_o (-)
11	200	80	17.5	0.3	0	13	0.47
7	150	70	17.5	0.3	0	13	0.47
6	50	70	17.5	0.3	0	13	0.47

Table 1 : Material properties for soil

Tunnel assembly	Shear retention factor	E (GPa)	F_t (kPa)	G_f (N/m)	γ (kN/m^3)	ν (-)
11	0.01	9	400	50	20.5	0.2
7	0.01	5	275	45	20.5	0.2
6	0.01	4.5	200	45	20.5	0.2

Table 2 : Material properties for masonry wall

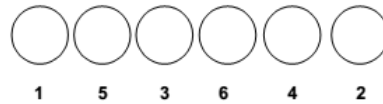


Figure 4 : Sequence of excavation for the 6-tunnel assembly

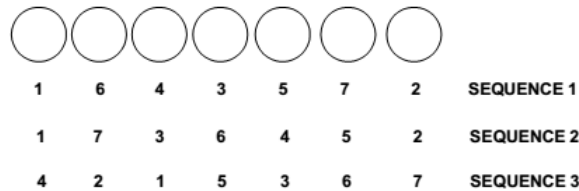


Figure 5 : Sequences of excavation for the 7-tunnel assembly

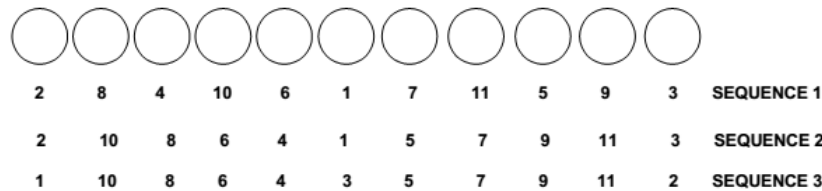


Figure 6 : Sequences of excavation for the 11-tunnel assembly

4 RESULTS

Results from different cases are looked at in terms of, on the one hand, the extent of damage, and, on the other hand, a set of different possible damage indicators or symptoms, observed in their respective evolution during the excavation process. The extent of damage is expressed by a measure of crack opening, either in mean or in maximum terms.

Many different observation variables are alternatively considered as possible damage indicators or symptoms, including: maximum angular strain, deflection ratio, maximum average horizontal strain, maximum differential settlement, tilt and maximum change in slope. Deflection ratio, maximum average horizontal strain and maximum angular strain have already been extensively used as damage indicators in the literature [13][6], whilst a correlation between the maximum change of slope and damage has not been presented yet to the best of the authors' knowledge. In the present work, no apparent correlation with damage has been found for tilt and maximum differential settlement, so results will be presented in terms of the following quantities only:

- Maximum average horizontal strain (ϵ_h), defined as the maximum change in length of wall at the foundation level over a distance of 1m;
- Maximum change in slope ($\Delta\theta$), defined as the maximum of the second derivative of the vertical settlement profile;
- Angular strain (β) and deflection ratio (DR), defined as explained in Figure 7;
- Maximum crack width (crack max) and mean crack width (crack mean).

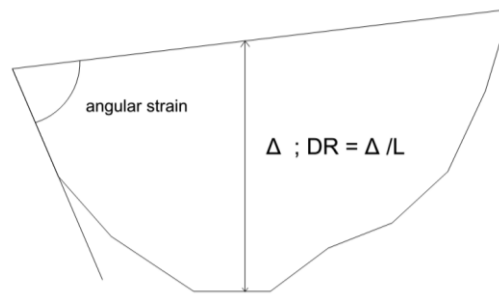


Figure 7: Angular strain (β) and deflection ratio (DR)

Analyses were carried out for the 6-, 7-, 11-tunnel assemblies. Only the 11-tunnels assembly is shown here, with two different opening configurations (one door and two doors) and different excavation sequence. Two different excavation sequences were considered for the case of opening configuration with one door. Results are reported in Figures 8-19. Figures in dotted lines depict the evolution of damage (in terms of maximum crack width) with the progression of excavation stages; figures in continuous lines present the damage-symptom correlation at each excavation stage. Unlike the previous cases, tunnel-related damage started from the first excavation in this case. This is due to the fact that the excavation process started from the central portion for both excavation sequences (see again Figure 6).

The last excavation stage inflicted much more damage than the other stages in excavation sequence 1, while the sixth excavation stage proved to be the one inducing most damage in excavation sequence 2. Overall, excavation sequence 2 inflicted much more damage than the excavation sequence 1.

The behaviour of wall is very different for the two excavation sequences. The only symptom showing a satisfactory correlation with damage for both sequences is $\Delta\theta$.

In the case of opening configuration with two doors, three different excavation sequences were considered in this case. Results are reported in Figures 20-31. The tunnel-related damage

started from the first excavation for sequence 1 and 2, while it started from the third excavation for sequence 3; excavation commenced from the outermost tunnels for sequence 3 (Figure 6).

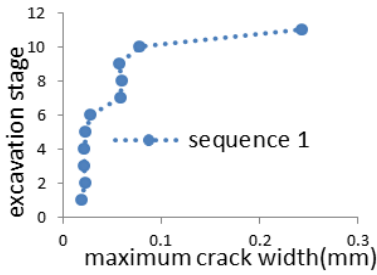


Figure 8: Crack max evolution

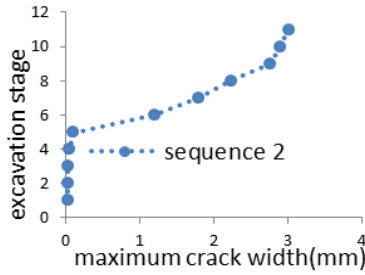


Figure 9: Crack max evolution

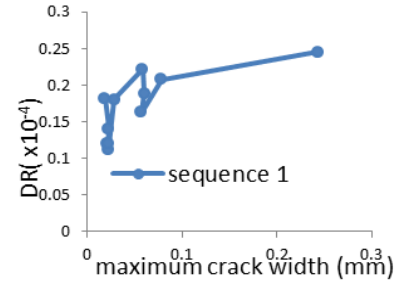


Figure 10: DR vs. crack max

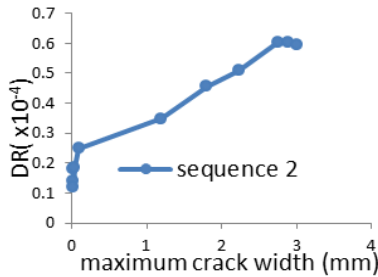
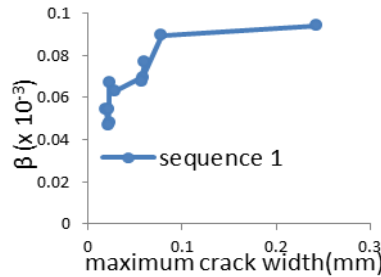
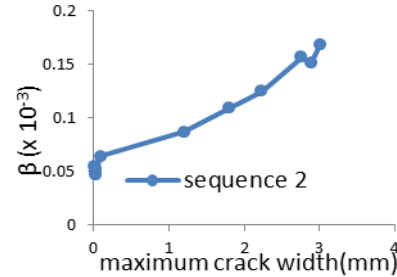
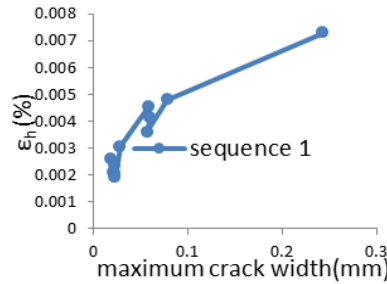
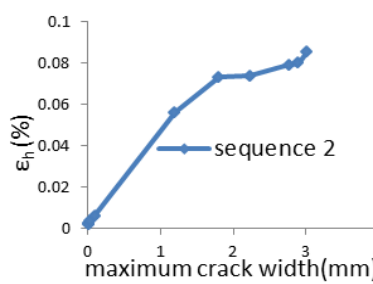
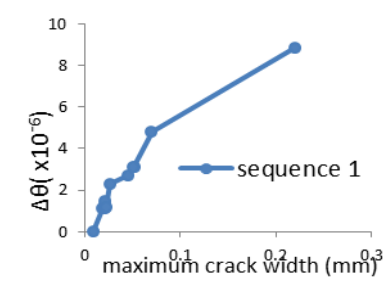
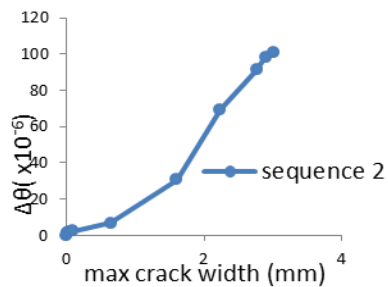
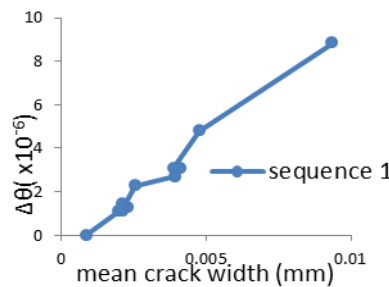
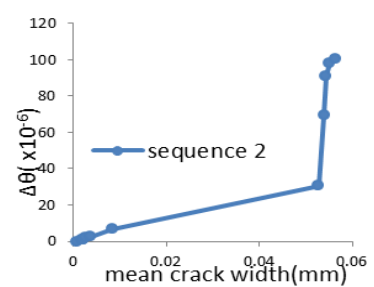


Figure 11: DR vs. crack max

Figure 12: β vs. crack maxFigure 13: β vs. crack maxFigure 14: ε_h vs. crack maxFigure 15: ε_h vs. crack maxFigure 16: $\Delta\theta$ vs. crack maxFigure 17: $\Delta\theta$ vs. crack maxFigure 18: $\Delta\theta$ vs. crack meanFigure 19: $\Delta\theta$ vs. crack mean

The sequence 2 inflicted much more damage than the other two sequences. Excavation sequence 3 can be adopted for this case along with β as damage-indicator. Excavation sequences 1 and 3 gave highly nonlinear and chaotic correlation between DR/ ε_h and maximum crack width; excavation sequence 2 resulted in regular nonlinear relationship between DR and ε_h ,

and fairly linear relationship between average horizontal strain and maximum crack width. The correlation between β and maximum crack width is almost similar for all three sequences.

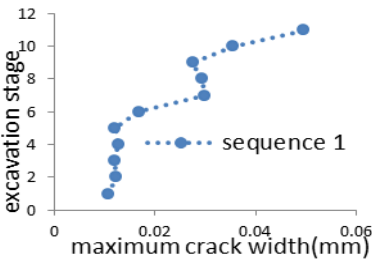


Figure 20 : Crack max evolution

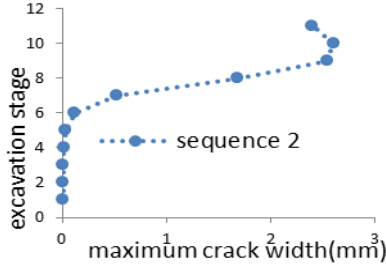


Figure 21 : Crack max evolution

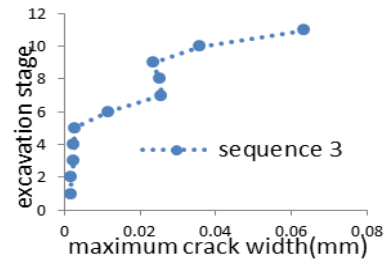


Figure 22 : Crack max evolution

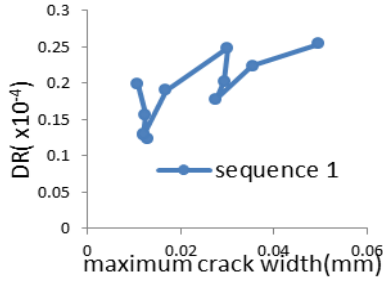


Figure 23 : DR vs. crack max

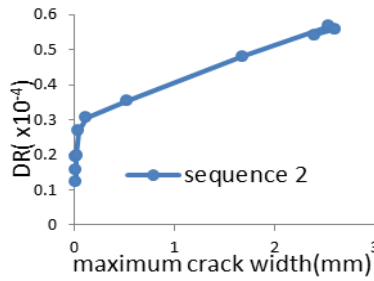


Figure 24 : DR vs. crack max

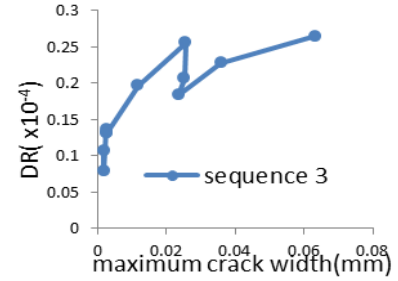
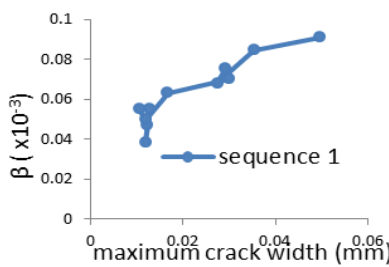
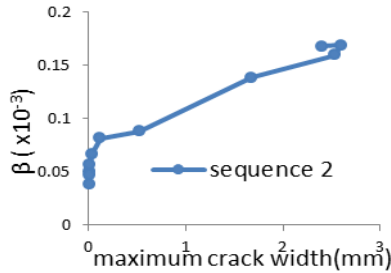
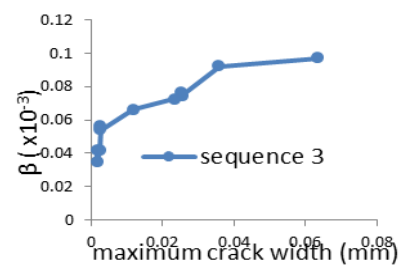
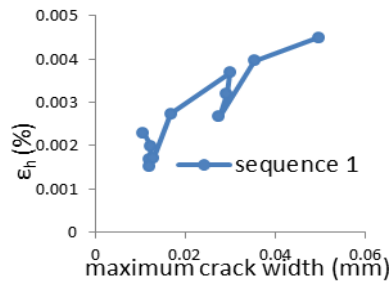
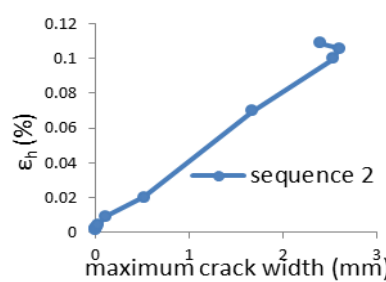
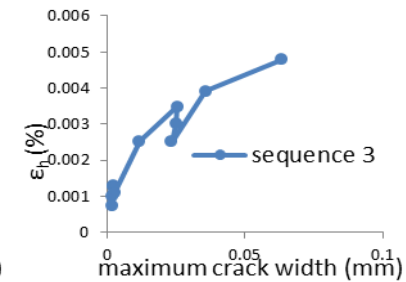


Figure 25 : DR vs. crack max

Figure 26 : β vs. crack maxFigure 27 : β vs. crack maxFigure 28 : β vs. crack maxFigure 29 : ϵ_h vs. crack maxFigure 30 : ϵ_h vs. crack maxFigure 31 : ϵ_h vs. crack max

5 CONCLUSIONS AND RECOMMENDATIONS

The present paper aimed at investigating how closely-spaced micro-tunnelling can inflict damage onto existing masonry buildings and how monitoring during construction can help to reduce the risk of damage. In the light of the results discussed above, the following conclusions can be drawn:

- For any given wall configuration/geometry, the extent of damage at the completion of the entire excavation process strongly depends on the excavation sequence. Damage is much less when excavation starts from outermost tunnels.
- In all simulated cases, if the proper excavation sequence is adopted in design, the maximum crack experienced during excavation is limited to values ranging from 0.05 to 0.35 mm depending on the case at hand; this can be regarded as a “very slight” damage according to the literature. This result is acknowledged to be strongly dependent on the geometric and mechanical parameters of the structure and the soil as well as on the design of micro-tunnels. In order to generalize this result, however, simulations need to be extended to include a wider range of mechanical/geometrical properties of soil and masonry. These preliminary results suggest the feasibility of the proposed, innovative base isolation system.
- Different possible damage indicators or symptoms have been monitored during simulations, some taken from the literature and others newly proposed. In general no simple correlation can be identified between damage and any particular symptom. No symptom appears to neatly prevail over the others in all explored simulation cases. On average, the best damage indicators, capable of well tracking damage evolution during construction, appear to be the maximum average horizontal strain, ϵ_h , and the maximum change in slope, $\Delta\theta$, which provide a nearly linear relationship with the maximum or the mean crack width in several cases. The worst damage indicators appear to be the tilt and the maximum differential settlement. These results suggest that “global” indicators based on the knowledge of few settlement values along the structure, which are typically monitored in common practice, are generally insufficient to reliably track the evolution of damage in a problem of closely-spaced multiple tunnels. “Local” indicators, unfortunately requiring a larger number of measurement points from closely-spaced sensors, appear much more representative of the actual damage extent in the present application. Image acquisition and processing monitoring systems (e.g. laser-scanner) or distributed fibre optic sensing technologies seem the most indicated to this purpose.

ACKNOWLEDGEMENTS

The Authors thank very much Dr. Badar Zeeshan for his very helpful contribution to this study.

REFERENCES

- [1] Clemente P., De Stefano A. (2011). "Application of seismic isolation in the retrofit of historical buildings". In Brebbia C.A. & Maugeri M. (eds) *Earthquake Resistant Engineering Structures*, 41-52, WIT Transactions on The Built Environment, Vol. 120, ISSN 1743-3509 (on line).
- [2] Clemente P., De Stefano A., Renna S. (2011). "Isolation system for existing buildings". *Proc., 12th World Conf. on Seismic Isolation, Energy Dissipation and Active Control of Structures - 12WCSI* (Sept. 20-23, Sochi, Russia).
- [3] Peck, R. D. (1969). "Deep excavations and tunneling in soft ground", *Proceeding 7th International conference on soil mechanics and foundation engineering*, (pp. 225-290).
- [4] O' Reilly, M. P. and New, B. M. (1982). "Settlements above tunnels in United Kingdom: their magnitude and prediction", *Proceeding of Tunneling* (pp. 55-64). Institute of Mining and Metallurgy, London.

- [5] Sagaseta, C. (1987). "Analysis of undrained soil deformation due to ground deformation", *Géotechnique*, 37, pp. 301-320.
- [6] Burland, J. B. and Wroth, C. P. (1974). "Settlement of buildings and associated damage", *Settlement of structures*, (pp. 611-654). Cambridge.
- [7] Rots, J. (1991). Numerical simulation of cracking in structural masonry. *HERON*, 36(2), pp. 49-63.
- [8] Rots, J. G. and Invernizzi, S. (2004). "Regularized sequentially linear saw-tooth softening model", *International Journal for Numerical and Analytical methods in Geomechanics*, 28, pp. 821-856.
- [9] Franzius, J. N., Potts, D. M. and Burland, J. B. (2006). "The response of structures to tunnel construction", *ICE- Journal of Geotechnical Engineering*, 159(1), 3-17.
- [10] Addenbrooke, T. I. and Potts, D. M. (2001). "Twin tunnel interaction-surface and subsurface effects", *International Journal of Geomechanics*, 1, pp. 249-271.
- [11] Sagaseta, C., Lopez, A., Gomez, J. and Pina, R. (1999). "Soil deformation due to the excavation of two parallel caverns", In F. B. Barends, J. Lindenberg and H. Luger (Ed.), 12th European Conference on Soil Mechanics and Geotechnical Engineering , (pp. 2125-2131). Amsterdam.
- [12] Chapman, D. N., Ahn, S. K., Hunt, D. and Chan, A. (2006). "The use of model test to investigate the ground displacements associated with multiple tunnel construction in soil", *Tunnelling and Underground Space Technology*, 21(3-4), pp. 413-413.
- [13] Boscardian, M. and Cording, E. J. (1989). "Building response to excavation-induced settlement", *ASCE-Journal of Geotechnical Engineering*, 115(1), 1-21.
- [14] Clemente, P., Bontempi, F. and De Stefano, A. (2012). "Application of seismic isolation in masonry buildings", *5th European conference on structural control*, (p. paper no. 117). Genoa, Italy.
- [15] Clemente, P., De Stefano, A. and Zago, R. (2012). "Seismic isolation in existing complex structures", *15th World Conference on Earthquake Engineering, paper No 712*. Lisbon.
- [16] DIANA Finite Element Analysis (2012). *User's Manual, Release 9.4.4*. TNO Building Construction & Research.
- [17] Zeeshan B.A., De Stefano A., Matta E. and Quattrone A. (2013). Monitoring of existing masonry buildings during construction of an innovative base-isolation system. Proc. 6th International Conference on Structural Health Monitoring of Intelligent Infrastructure, Hong Kong, 9-11 December 2013.